Volume 333, number 1,2, 197–202 FEBS 13172 October 1993

Kinetic and structural characterization of an intermediate in the biomineralization of bacterioferritin

Nick E. Le Brun[a], Michael T. Wilson[b], Simon C. Andrews[c], John R. Guest[c], Pauline M. Harrison[c], Andrew J. Thomson[a,*], Geoffrey R. Moore[a]

[a]*Centre for Metalloprotein Spectroscopy and Biology, School of Chemical Sciences, University of East Anglia, Norwich, NR4 7TJ, UK*
[b]*Department of Chemistry and Biological Chemistry, University of Essex, Colchester, CO4 3SQ, UK*
[c]*The Krebs Institute, Department of Molecular Biology and Biotechnology, University of Sheffield, Sheffield, S10 2TN, UK*

Received 23 August 1993; revised version received 14 September 1993

The mechanism by which iron-storage proteins take up and oxidise iron(II) is not understood. We show by rapid-kinetic and EPR measurements that iron uptake, in vitro, by a bacterial iron-storage protein, bacterioferritin, involves at least three kinetically distinguishable phases: phase 1, the binding of Fe(II) ions, probably at a dimeric iron ferroxidase centre; phase 2, oxidation of the Fe(II) dimer and production of mononuclear Fe(III); and phase 3, iron core formation.

Bacterioferritin; Iron-uptake; Kinetic phase; Iron(II) dimer

1. INTRODUCTION

The formation of non-haem iron cores by the iron-storage proteins ferritin [1–8] and bacterioferritin [9–11], of magnetite particles by magnetotactic organisms [12–14], and of goethite- and lepidocrocite-containing teeth by marine organisms [15], is a subject of considerable biological and chemical interest. Investigations of these biominerals focus on their relationship with the iron metabolism of their respective organisms, on the use of their organic components for the synthesis of novel inorganic materials [16], and on the development of inorganic syntheses which mimic physical aspects of the metal-containing component of the biomineral [17,18]. Such studies are handicapped by a lack of information about the biochemical mechanisms of biomineral formation.

The bacterioferritin (BFR) of *E. coli*, is an iron-storage protein consisting of 24 identical polypeptide chains (M_r 18,500) which pack to form a highly symmetrical, approximately spherical, protein shell surrounding a central 8 nm cavity, in which large amounts of iron can be stored. The *bfr* gene of *E. coli* has been cloned, sequenced and overexpressed to produce BFR at 15% of cell protein [19,20]. Secondary structure prediction and molecular modelling point to a close structural similarity between BFR and mammalian ferritin [10,21]. A major difference between the two is that the bacterioferritins contain up to 12 haem *b* groups, each coordinated by 2 methionine residues [22], whilst the ferritins, as isolated, do not contain haem.

Iron-uptake studies with iron-free (apo) ferritin, employing a ferrous salt and an appropriate oxidant (usually molecular oxygen), show that ferritin is able to catalyse the oxidation of iron(II) to iron(III) [1,2]. Mammalian ferritin is composed of two subunit types, known as H and L. Core reconstitution studies of recombinant H- and L-chain proteins have shown that this catalytic function, the ferroxidase activity, is associated solely with the H-subunit [23]. The ferroxidase centre of H-chain ferritin is thought to be located at a metal binding site, occupied by Tb(III) or Ca(II) in the crystal structure, which is assumed to be capable of binding iron [6]. The effects of site-directed mutagenesis give support to this proposal [3,7,24]. A model in which a μ-oxo bridged Fe(III) dimer is formed at the ferroxidase centre has been proposed [25]. Mössbauer spectra of ferritin under conditions of low iron loading support the existence of such a dimer, whereas site-directed variants, in which oxidation is slow, give no evidence for dimer formation [7]. However, the kinetic characteristics of iron uptake by ferritin have yet to be fully explored. Studies of iron uptake by apo-BFR are more limited than those with apo-ferritin and detailed mechanistic proposals have not been made for BFR. The studies with BFR reported here give clear experimental support for the formation of iron(II) dimers at centres in the protein at which oxidation occurs. Since the data show that ~ 50 Fe(II) can bind in this way, it is proposed that each of the 24 subunits of BFR contain a ferroxidase centre binding two Fe(II) atoms. Evidence is also

*Corresponding author. Fax: (44) (60) 325-9396.

provided for three kinetically distinguishable phases in the iron uptake process, termed in order of occurrence, phases 1, 2 and 3. The most rapid of these, phase 1, is monitored through a perturbation of the ferric haem *b* spectrum, while phases 2 and 3 are monitored by the absorption associated with non-haem Fe(III).

2. MATERIALS AND METHODS

2.1. *Preparation of apo-*E. coli *BFR*

BFR was isolated from the over-producing strain, *E. coli* JM101 (pGS281), as described previously [26]. Apo-BFR was prepared by dialysing BFR against 0.12 M thioglycolic acid in 0.1 M sodium acetate, pH 5.0. The dialysate was exchanged twice over 72 h. Thioglycolic acid was removed by dialysing the protein against 25 mM sodium phosphate, pH 7.0, for 48 h, during which the dialysate was exchanged three times. Apo-BFR was subsequently exchanged into 100 or 200 mM MES buffer, pH 6.5, using an ultrafiltration unit (Amicon) fitted with a PM 30 membrane operating at a pressure of 55 psi. Each stage of the preparation was carried out at 4°C. The iron content of apo-BFR determined by atomic emission spectroscopy was approximately 1 iron per 24 subunits, in addition to the 10 haem iron atoms present per 24 subunits.

2.2. *Addition of iron(II) to apo-BFR*

Solutions of ferrous ammonium sulphate were freshly prepared prior to each experiment by dissolving weighed amounts of the salt in Analar grade water, previously deoxygenated by bubbling with argon or nitrogen gas for at least 1 h. Kinetic measurements of changes in absorption on addition of iron(II) to apo-BFR were measured either by a conventional UV-visible spectrophotometer (Aminco DW-2000), for which additions to the continuously stirred sample were made using a micro-syringe (Hamilton); or by a stopped-flow apparatus (Applied Photophysics DX17MV).

2.3. *Reduction of iron(III) to iron(II) and addition of gaseous nitric oxide*

Selective reduction of non-haem, non-core iron(III) was achieved by the addition of excess sodium ascorbate as previously described [11]. Nitric oxide gas was added to solutions of BFR under anaerobic conditions to avoid side reactions of NO and O_2, as previously described [11].

2.4. *EPR measurements*

EPR spectra were measured with an X-band spectrometer (Bruker ER200D with an ESP 1600 computer system) fitted with a liquid helium flow cryostat (Oxford Instruments plc, ESR9). Concentrations of the iron(II)–iron(II)[NO] complex were estimated by double integration of the EPR spectrum and comparison with the doubly integrated spectrum of a known concentration of an aqueous copper(II) EDTA complex [27].

3. RESULTS AND DISCUSSION

3.1. *Kinetics*

Iron uptake by *E. coli* BFR was investigated by adding ferrous ammonium sulphate to aerobic solutions of apo-BFR and monitoring changes in absorption over the range 380–450 nm, associated with the haem groups, and changes in absorption at 340 nm, associated with the oxidation of Fe(II) to Fe(III), as a function of time.

The fastest phase of the iron uptake process (phase 1) with $t_{1/2} \sim 50$ ms (1 mg apo-BFR/ml, 112 μM Fe(II) at 30°C) was detected in the 380–450 nm region, after the aerobic addition of 50 Fe(II) ions per BFR molecule. This region is dominated by the haem Soret band transitions. The absorbance changes showed a perturbation of the haem Soret band consistent with a blue shift of less than 1 nm (Fig. 1A). This was not due to a change in the redox state of the haem group since haem reduction would lead to a 8 nm red shift of the Soret band and large absorption changes ($\Delta A > 0.1$). Hence it was concluded that BFR haem does not cycle its redox state during the oxidation of iron(II). The maximum absorbance change of phase 1 was observed after 50 or more Fe(II) ions per BFR molecule had been added, indicating that the Fe(II) binding sites of BFR were saturated. The shift in the haem Soret peak most probably arises from a minor perturbation of the haem binding pocket consequent upon the uptake of 1 or 2 Fe(II) ions per protein subunit.

Phase 1 absorbance changes gave a pseudo-first order rate constant of 13 s^{-1} (0.5 mg apo-BFR/ml, 55 μM Fe(II) at 30°C). The linear relationship given in Fig. 1B showed a first-order dependence of the pseudo-first-order rate constant on iron concentration, and gave an apparent second-order rate constant of 2.5×10^5 $M^{-1} \cdot s^{-1}$.

Oxidation of the non-haem Fe(II) was monitored at 340 nm. The addition of up to 400 Fe(II) ions per BFR molecule caused a time dependent increase of absorption at 340 nm with two distinct phases (Fig. 2): the first (phase 2) lasting only a few seconds was followed by a slower phase (phase 3) lasting up to 30 min. Additions of varying amounts of Fe(II) ions to apo-BFR showed that iron oxidation during phase 2 became saturated at approximately 50 Fe(II) ions per BFR. Iron added in excess of 50 Fe(II) ions per BFR contributed to phase 3. In the absence of oxygen no increase in absorbance at 340 nm occurred upon the addition of Fe(II) to apo-BFR.

Phase 2 was further investigated by a series of stopped-flow experiments. The addition of Fe(II) to apo-BFR in aerobic solutions resulted in an exponential increase in absorption at 340 nm over the first 20 s (Fig. 3A). The maximum amplitude of the change increased linearly until approximately 50 Fe(II) ions per BFR molecule had been added (Fig. 3B). These observations imply that two Fe(II) ions per subunit are required to saturate phase 2. It is therefore proposed that the initial fast increase in absorption at 340 nm (phase 2) is due to the relatively rapid oxidation of iron at dimer sites situated within the ferroxidase centres, and that a maximum of 24 such iron dimers can be formed.

The slow increase in absorption at 340 nm identified as phase 3, is observed after the addition of 100, 200, and 400 Fe(II) ions per BFR molecule (Fig. 2). This corresponds to the build up of an iron core. Higher ratios of iron to protein gave rise to increasingly sigmoidal curves of absorbance against time. This is consistent with oxidation occurring at a growing core sur-

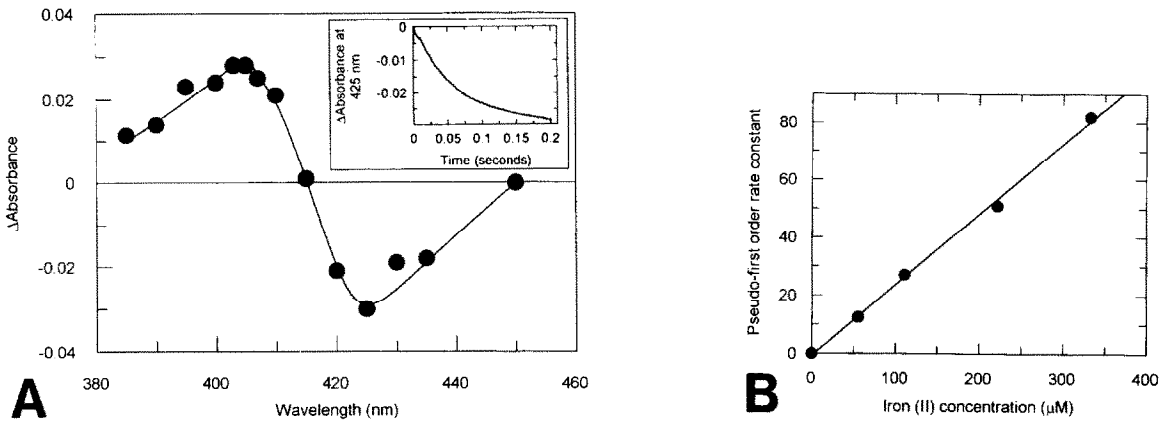

Fig. 1. (A) The amplitudes of absorbance changes measured by the stopped-flow method at 0.2 s after the addition of 50 Fe(II) ions per apo-BFR molecule, are plotted against the wavelength at which data was acquired. The protein concentration after mixing was 2.25 μM in 100 mM MES (2-[*N*-morpholino]ethanesulfonic acid) buffer pH 6.5, 30°C. The inset shows one representative measurement of absorbance (425 nm) after the addition of 50 Fe(II) ions per apo-BFR as a function of time. (B) A plot of phase 1 pseudo-first-order rate constants (30°C) measured at 425 nm as a function of Fe(II). Protein concentration after mixing was 1 μM; iron(II) concentrations are those after mixing.

face, because the rate of oxidation should increase in proportion to the core surface area, but become limited either by the remaining iron concentration (as in this case), or by the finite size of the iron-storage cavity. The simultaneous participation of a mechanism involving a protein catalytic centre in this slow phase is not precluded by the data.

Phase 2 was only observed with completely non-haem-iron-free BFR. Further additions of Fe(II) ions to aerobic solutions of apo-BFR containing 50 or more Fe(II) ions per BFR 3 h and 24 h after the initial addition of Fe(II) only exhibited a phase 3 change. This is illustrated in Fig. 4 for the addition of a further 100, 200, 300 and 400 Fe(II) ions per BFR 3 h after an initial treatment with 100 Fe(II) ions. These observations indicate that ferroxidase centres are not rapidly regenerated.

In summary, the kinetic data reported here indicate that iron uptake by apo-BFR proceeds by three distinct phases: the rapid binding of ~ 50 ferrous ions at specific protein sites (phase 1); the subsequent oxidation of ~ 50 ferrous ions by molecular oxygen (phase 2); and, eventually, growth of the iron core (phase 3).

A tyrosinate–Fe(III) complex giving rise to a charge transfer band at 550 nm was recently reported as a transient species observed after the addition of Fe(II) to recombinant bullfrog red cell H-chain ferritin [28], and subsequently observed to form under similar conditions in recombinant human H-chain ferritin [24]. Measurements of absorption in the 550 nm region after the addition of 50 Fe(II) ions per apo-BFR molecule, under conditions of protein and iron concentration which allowed the detection of the tyrosinate–Fe(III) complex in bullfrog red cell and human H-chain ferritins, showed that this complex is not formed in *E. coli* BFR.

3.2. *EPR spectroscopy*

EPR spectroscopy has been used previously [10,11] to identify four different chemical forms of non-haem iron in *E. coli* BFR, namely, mononuclear high-spin Fe(III), mononuclear Fe(II), dimeric Fe_2(II), and a ferric form of nucleated core. The mononuclear iron species are thought to arise from the partial occupancy of dimeric iron sites situated in each protein subunit [10,11]. The detection of Fe(II) ions requires the addition of the spin label NO, which forms nitrosyl complexes with Fe(II) ions to generate either [Fe(II)NO] with spin S = 3/2, and g-values in the region of $g \sim 4$; or [Fe_2(II)NO] with spin S = 1/2, and g-values close to 2.0.

The EPR spectrum of an aerobic sample of apo-BFR frozen approximately 2 min after the addition of 50 Fe(II) ions per BFR molecule contains, in addition to the haem group resonances at g = 2.88, 2.31, and 1.46 [22], a high intensity signal at g = 4.28 (Fig. 5a). This

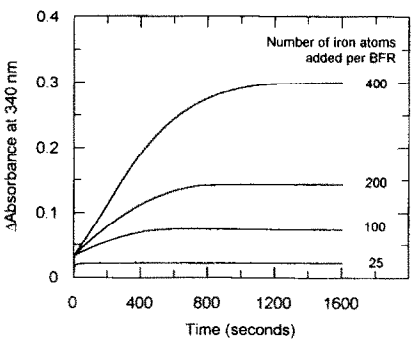

Fig. 2. Absorption change measured at 340 nm after the addition of 25, 100, 200 and 400 Fe(II) ions per apo-BFR molecule. Iron(II) was added as a 50 mM solution of ferrous ammonium sulphate to 0.5 μM (approx. 0.23 mg/ml) solutions of apo-BFR in 100 mM MES, pH 6.5, 30°C.

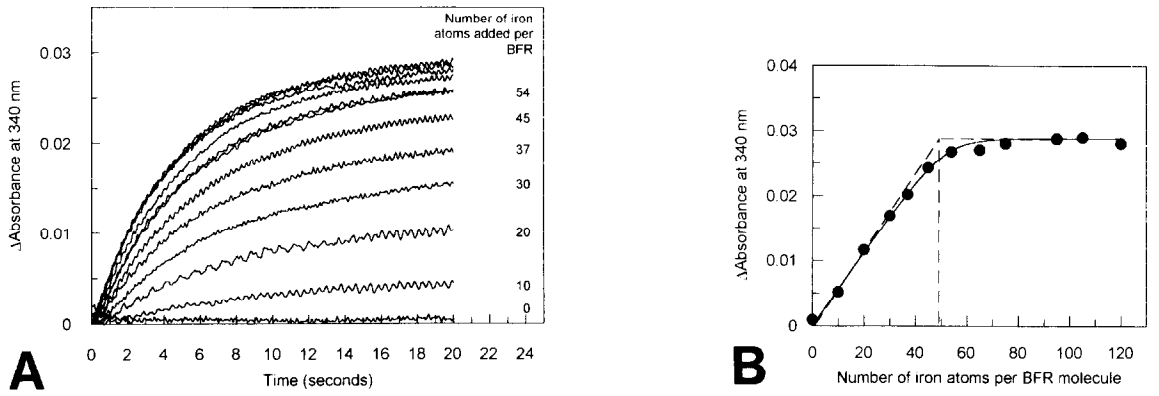

Fig. 3. (A) Stopped flow experiments monitoring absorption at 340 nm after the addition of 0, 10, 20, 30, 37, 45, 54, 65, 75, 95, 105 and 120 Fe(II) ions per apo-BFR. Iron was added as a solution of ammonium ferrous sulphate. The apo-BFR concentration in 100 mM MES buffer, pH 6.5, 30°C after mixing was 0.4 μM. (B) A plot of absorption increase at 340 nm measured after 20 s against the number of iron atoms added per apo-BFR.

indicates that a significant proportion of the added iron(II) is present as mononuclear high spin $S = 5/2$ iron(III). Virtually complete reduction of the non-haem iron(III) species to EPR inactive iron(II), and the corresponding loss of signal intensity at $g = 4.28$, was achieved by the addition of excess sodium ascorbate to a similar sample prior to freezing. The subsequent addition of nitric oxide gas to the ascorbate-reduced sample yielded the EPR spectrum of Fig. 5b. The spectrum contains traces of two $S = 3/2$ mononuclear iron(II) complexes of nitric oxide (Fe(II)[NO]) at $g = 4.36$ and 3.69; and $g = 3.98$ respectively [11], together with the haem group resonances of unaffected intensity. The high intensity signal at $g = \sim 2$ is shown in greater detail in Fig. 5c. The g-values of 2.05, 2.02 and 2.01 are similar to those previously assigned to an [Fe(II)Fe(II)NO] species [11]. These signals arise either from the antiferromagnetic coupling of two $S = 2$ high spin ferrous ions, to give a $S = 0$ ground state coupled with a $S = 1/2$ nitric oxide; or from antiferromagnetic coupling of $S = 2$ Fe(II) and $S = 3/2$ Fe(II)NO, both possibilities leading to systems having $S = 1/2$ ground states. Estimation of the concentration of the $S = 1/2$ species indicated that there are 8 [Fe(II)Fe(II)NO] dimers per BFR molecule. The anaerobic addition of 50 Fe(II) ions per apo-BFR molecule in the presence of excess ascorbate, followed by treatment with NO, gave the EPR iron dimer signal with an integrated intensity of approximately 22 dimers per BFR molecule.

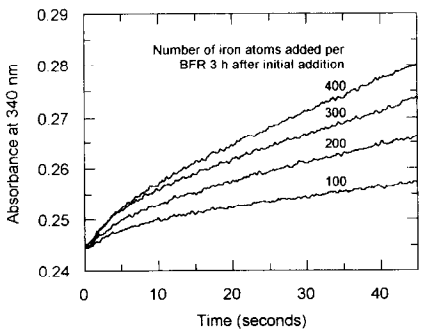

Fig. 4. Absorption change at 340 nm measured after the addition of 100, 200, 300 and 400 Fe(II) ions per BFR molecule, 3 h after an initial addition of 100 Fe(II) ions per apo-BFR molecule.

3.3. *Mechanism of core formation*

Ferritin core formation, in vitro under aerobic conditions, proceeds via a complex process, characterised by at least two distinct phases [1,2]. In one of the phases the ferroxidase centre is thought to promote nucleation of the core at specific sites on the inner protein surface; and in the other, the site of oxidation switches to the surface of the growing crystallite. Both phases involve the transfer of electrons to oxygen, but with significant differences in stoichiometry: the initial stage involves two electron reduction of oxygen to hydrogen peroxide whereas the subsequent oxidation of iron at the core surface involves a four electron reduction of oxygen [29]. There must be an Fe(II) binding phase prior to oxidation but this has not previously been detected because Fe(II) ions have only weak or non-existent absorption bands in the visible region. The present work provides the first evidence for three distinct kinetic phases in the ferroxidase process in *E. coli* BFR using optical methods, including detection of the Fe(II) binding phase.

The presence of the haem groups, approaching one per two subunits, provides an internal optical reporter for Fe(II) binding at ferroxidase centres. The high intensity of the haem Soret band coupled with its sensitivity to Fe(II) binding allowed the rate of this process, phase 1, to be monitored (Fig. 1). This was much faster than the oxidation of Fe(II) at the ferroxidase centres, phase 2 (Figs. 2 and 3). The Fe(II)-dependence of phase 2 is linearly related to Fe(II) concentration, up to a maximum loading of ~ 50 Fe(II) ions per protein molecule (Fig. 3B). This suggests either that single Fe(II) oxidation at ferroxidase centres occurs at low iron concentra-

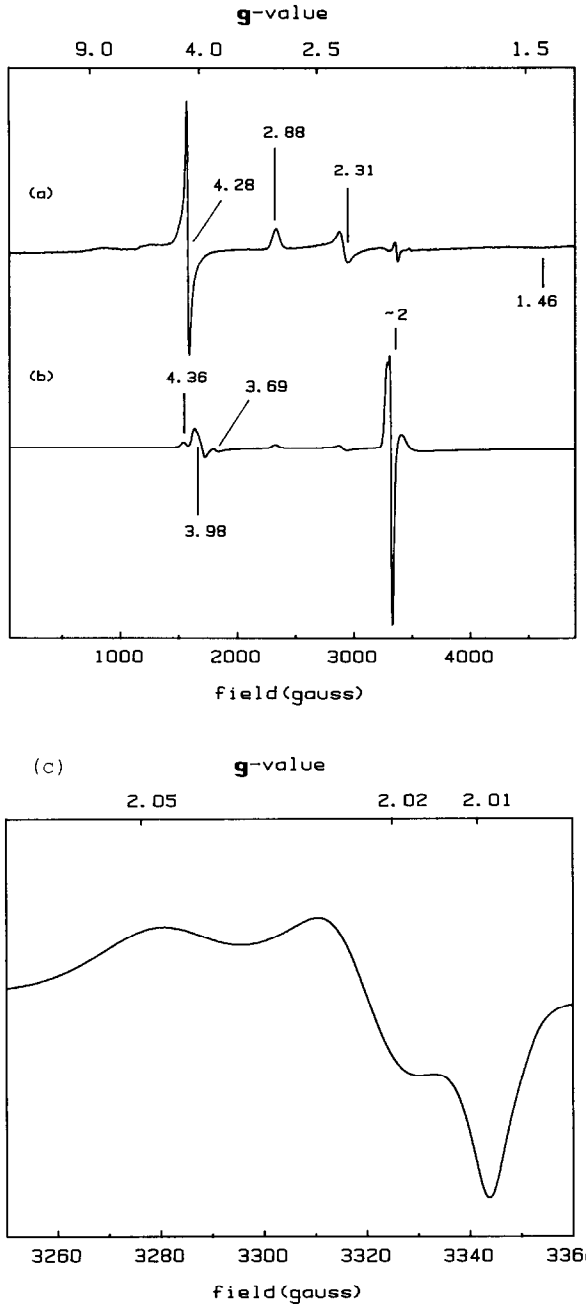

Fig. 5. X-band EPR spectra of 9 μM *E. coli* BFR in 200 mM MES buffer, pH 6.5. (a) Sample was frozen approximately 2 min after the addition of 50 iron atoms per BFR. Conditions: modulation amplitude 10 GHz, frequency 100 kHz; microwave frequency 9.38 GHz; power 2.01 mW; Temperature 10 K. (b) Sample similar to that in Fig. 5a after reduction of non-haem iron by the addition of sodium ascorbate solution, and treatment with nitric oxide gas. The feature at approximately $g = 1.9$ is due to excess nitric oxide in solution. Measurement conditions were the same as in Fig. 5a except that the gain was a factor of 0.125. (c) Sample and conditions as in Fig. 5b, except for temperature 40 K.

tions, or that the initial Fe(II) binding step is both rapid and weak. In the latter case the on and off rates of Fe(II) are fast, such that oxidation only occurs when the dimeric centre is filled. Thus, even at low concentrations of Fe(II) there is a significant probability that a ferroxidase centre is occupied by 2 Fe(II) ions and that oxidation can proceed.

The binding of NO to Fe(II) sites in proteins often mimics the binding of O_2 [30]. Hence, the use of NO as a spin probe not only allows the detection of an Fe(II) dimer in BFR (Fig. 5), but also indicates that a single O_2 molecule binds to the two Fe(II) ions at the ferroxidase centre. Hence, the oxidation of Fe(II) by dioxygen in phase 2 probably proceeds by a 2-electron process generating hydrogen peroxide, and, although there are other possibilities, a simple mechanism in which 2 Fe(II) ions bind at the ferroxidase centre prior to oxygen binding and electron transfer is preferred.

The EPR data indicate that a significant fraction of the iron is present as monomeric Fe(III) after Fe(II) oxidation. This suggests that there is a significant oxidation of single Fe(II) ions, or that the dimers formed by oxidation at the ferroxidase centres break down. The latter interpretation is preferred, because approximately 50 Fe(II) ions are required to saturate phase 2, and because the addition of 50 Fe(II) ions per BFR yields almost complete dimer occupation of the ferroxidase centres in the absence of dioxygen.

The observation that phase 2 is only detected when BFR is completely non-haem-iron-free (Fig. 4), coupled with the demonstration by EPR that oxidation at the ferroxidase centres yields monomeric Fe(III) ions, is an important guide to the overall process of iron uptake and core formation. A plausible model, in which at least one of the monomeric Fe(III) ions formed by oxidation partially blocks and prevents regeneration of the ferroxidase centre, can be proposed. The second Fe(III) could then form part of the nucleating centre for core formation. There are many variants of this scheme, but an essential feature of all would be that the ferroxidase centres need only to be turned over once, because thereafter the nucleated core surface would form the site of oxidation.

Acknowledgements: We thank The Wellcome Trust for support via a project grant and a Prize Studentship awarded to N.L.B., and the SERC for supporting the UEA Centre for Metalloprotein Spectroscopy and Biology and for an Advanced Fellowship awarded to S.C.A. M.T.W. thanks Delta Biochemistry for support in purchasing the stopped-flow spectrophotometer (DX17MV Applied Photophysics). G.R.M. thanks Prof. E.C. Theil and Dr. G.S. Waldo (NCSU, USA) for stimulating discussions on Fe uptake into ferritins, prompted in part by their observation of a fast phase of iron uptake associated with 48 irons entering tadpole ferritins.

REFERENCES

[1] Macara, I., Hoy, T.G. and Harrison, P.M. (1972) Biochem. J. 126, 151–162.
[2] Bryce, C.F.A. and Crichton, R.R. (1973) Biochem. J. 133, 301–309.
[3] Lawson, D.M., Treffry, A., Artymuik, P.J., Harrison, P.M., Yewdall, S.J., Luzzago, A., Cesareni, G., Levi, S. and Arosio, P. (1989) FEBS Lett. 254, 207–210.

[4] Rohrer, J.S., Frankel, R.B., Papaefthymiou, G.C. and Theil, E.C. (1989) Inorg. Chem. 28, 3393–3395.
[5] Hanna, P.M., Chen, Y. and Chasteen, N.D. (1991) J. Biol. Chem. 266, 886–893.
[6] Lawson, D.M., Artymuik, P.J., Yewdall, S.J., Smith, J.M.A., Livingstone, J.C., Treffry, A., Luzzago, A., Levi, S., Arosio, P., Cesareni, G., Thomas, C.D., Shaw, W.V. and Harrison, P.M. (1991) Nature 349, 541–544.
[7] Bauminger, E.R., Harrison, P.M., Hechel, D., Nowik, I. and Treffry, A. (1991) Biochim. Biophys. Acta 1118, 48–58.
[8] Sun, S. and Chasteen, N.D. (1992) J. Biol. Chem. 267, 25160–25166.
[9] Watt, G.D., Frankel, R.B., Jacobs, D., Huang, H. and Papaefthymiou, G.C. (1992) Biochem. 31, 5672–5679.
[10] Cheesman, M.R., Le Brun, N.E., Kadir, F.H.A., Thomson, A.J., Moore. G.R., Andrews, S.C., Guest, J.R., Harrison, P.M., Smith, J.M.A. and Yewdall, S.J. (1993) Biochem. J. 292, 47–56.
[11] Le Brun, N.E., Cheesman, M.R., Thomson, A.J., Moore, G.R., Andrews, S.C., Guest, J.R. and Harrison, P.M. (1993) FEBS Lett. 323, 261–266.
[12] Blakemore, R.P. (1982) Annu. Rev. Microbiol. 36, 217–238.
[13] Mann, S., Frankel, R.B. and Blakemore, R.P. (1984) Nature 310, 405–407.
[14] Fassbinder, J.W.E., Stanjek, H. and Vali, H. (1990) Nature 343, 161–163.
[15] Webb, J., Macey, D.J. and Mann, S. (1989) in: Biomineralisation (Mann, S., Webb, J. and Williams, R.J.P. eds.) pp. 345–387, UCH Publishers.
[16] Meldrum, F.C., Wade, V.J., Nimmo, D.L., Heywood, B.R. and Mann, S. (1991) Nature 349, 684–687.
[17] Heath, S.L. and Powell, A.K. (1992) Angew Chemie 31, 191–193.
[18] Taft, K.L., Papaefthymiou, G.C. and Lippard, S.J. (1993) Science 259, 1302–1305.
[19] Andrews, S.C., Smith, J.M.A., Guest, J.R. and Harrison, P.M. (1989) Biochem. Biophys. Res. Commun. 158, 489–496.
[20] Andrews, S.C., Harrison, P.M. and Guest, J.R. (1989) J. Bacteriol. 171, 3940–3947.
[21] Ford, G.C., Harrison, P.M., Rice, D.W., Smith, J.M.A., Treffry, A. and Yariv, J. (1984) Phil. Trans. R. Soc. Lond. B Biol. Sci. 304, 551–565.
[22] Cheesman, M.R., Thomson, A.J., Greenwood, C., Moore, G.R. and Kadir, F. (1990) Nature 346, 771–773.
[23] Levi, S., Luzzago, A., Cesareni, G., Cozzi, A., Franceschinelli, F., Albertini, A. and Arosio, P. (1988) J. Biol. Chem. 263, 18086–18092.
[24] Bauminger, E.R., Harrison, P.M., Hechel, D., Hodson, N.W., Nowik, I., Treffry, A. and Yewdall, S.J. (1993) Biochem. J. (in press).
[25] Treffry, A., Hirzmann, J., Yewdall, S.J. and Harrison, P.M. (1992) FEBS Lett. 302, 109–112.
[26] Andrews, S.C., Findlay, J.B.C., Guest, J.R., Harrison, P.M., Keen, J.N. and Smith, J.M.A. (1991) Biochim. Biophys. Acta 1078, 111–116.
[27] Aasa, R. and Vänngård, T. (1975) J. Magn. Res. 19, 308–315.
[28] Waldo, G.S., Ling, J., Sanders-Loehr, J. and Theil, E.C. (1993) Science 259, 796–798.
[29] Xu, B. and Chasteen, N.D. (1991) J. Biol. Chem. 266, 19965–19970.
[30] Nocek, J.M., Kurtz Jr., D.M., Sage, J.T., Debrunner, P.G., Maroney, M.J. and Que Jr., L. (1985) J. Am. Chem. Soc. 107, 3382–3384.